Mass Transfer to a Rotating Fluid:

Part I. Transport from a Stationary Disk to a Fluid in Bödewadt Flow

Solutions are developed for mass transfer between a fluid undergoing solid body rotation and a coaxial disk which is located on a stationary infinite surface. The fluid mechanics corresponds to a laminar Bödewadt boundary layer. The overall mass transfer is dominated by the outer portion of the disk, a result of the high transfer rate associated with a leading edge. The concentration field near the axis of rotation extends to great axial distances as a long narrow plume. Approximate analytical solutions are given for each of these regions, and a numerical solution is provided for the entire concentration field.

KENNETH A. SMITH and CLARK K. COLTON

Department of Chemical Engineering
Massachusetts Institute of Technology
Cambridge, Massachusetts 02139

SCOPE

Axially symmetric boundary layers in laminar, incompressible Newtonian flow are of special interest in fluid dynamics because they frequently occur in real situations and because exact solutions of the Navier-Stokes or boundary layer equations are obtainable in some cases. A classical example is the case of flow in the neighborhood of a disk which rotates in a large body of quiescent fluid. Heat and mass transfer from such a rotating disk is of both theoretical interest and practical utility, for example, in the experimental study of transport and kinetic phenomena, because the rotating disk is a surface of uniform accessibility such that the concentration profile is independent of distance from the axis of rotation.

A problem closely connected with the rotating disk is its inverse, namely, the case of motion near a stationary surface when the fluid at a large distance above it is in solid body rotation. Near the surface, flow is radially inwards and axially upwards. An exact solution to the boundary layer equations for this problem has been obtained by Bödewadt (1940). Heat and mass transfer under these conditions is of interest for several reasons. The solution gives physical insight into the two-dimensional interaction between convection and diffusion because marked differences in length scales characterize different regions of the concentration field and because convection normal to the surface plays an important role in the transport process. Further, the problem provides a distinct contrast to the rotating disk configuration in that, for boundary conditions of practical interest, the surface is not uniformly accessible. Most significantly, the problem has practical application, for example, to problems involving rotating turbo-machinery and vortex chambers. Application of the theory developed here to mass transfer from the base of an agitated cylindrical tank is treated in a companion paper (Colton and Smith, 1972).

The system of interest here consists of a body of fluid which undergoes solid body rotation at a large distance from an infinite stationary surface. A finite disk coincident with the surface and coaxial with the axis of rotation exchanges mass with the fluid, and it is assumed that a single ambient concentration exists at infinite distance from the disk surface. On the disk, boundary conditions of uniform concentration, uniform mass flux, and a permeable wall are considered. A theoretical solution for the concentration profile and mass transfer rate is obtained by a variety of techniques. The simplifications attendant to the rotating disk problem no longer hold, and it is necessary to solve the complete two-dimensional convective diffusion equation. A numerical solution for the entire concentration field is obtained by finite difference techniques for Schmidt numbers ranging from 10^{-1} to 10^{5}, and approximate analytical solutions are derived which are valid over regions for which one or more of the terms in the convective diffusion equation may be neglected.

For high Schmidt number, the developing concentration boundary layer near the (circular) leading edge is imbedded well within the momentum boundary layer. The axial convection and radial diffusion terms are neglected, and the velocity components are represented by the leading term in their Maclaurin expansions. This leads to Leveque-type similarity solutions for both constant concentration and constant flux boundary conditions on the disk. The region far from the surface is simplified if the product of the Schmidt number and the square root of the Reynolds number is large; in this case, the length scale associated with the axial direction is far greater than that for the radial direction, and lines of constant concentration are almost purely axial. These concepts lead to a particularly simple similarity solution which is asymptotically valid far from the surface. For a slightly modified radial boundary condition, an exact analytical solution is found in terms of the analogous transient conduction problem. Conversely, if the product of the Schmidt number and the square root of the Reynolds number is very small, the problem reduces to one of pure diffusion over virtually the entire concentration field.

CONCLUSIONS AND SIGNIFICANCE

For high Schmidt number, the leading edge solution, Equation (23), is an adequate representation of the concentration field over roughly the outer 20% of the disk. In this region, mass is convected radially inwards and diffused axially upwards, leading to a surface of highly nonuniform accessibility. The concentration field very close to the surface is relatively insensitive to the region of oscil-

Correspondence concerning this paper should be addressed to K. A. Smith.

latory flow which lies somewhat above it and which gives rise to coincident oscillations in the concentration profile (Figures 7 and 8). The oscillations decay rapidly with increasing distance from the disk and the resulting field at the edge of the momentum boundary layer forms the starting condition for development of the concentration field far from the surface. This field propagates for immense axial distances in the form of a plume (Figure 11) which, as it is depleted by radial diffusion, eventually becomes insensitive to the detailed field close to the surface. That is to say, it forgets its initial condition.

The mass transfer coefficient, calculated from the near-field numerical and leading edge solutions, is infinite at the leading edge and decreases rapidly as the distance from the axis decreases (Figure 3). The overall transport process is effectively dominated by the leading edge, the solution for which leads to an adequate representation of the average mass transfer coefficient for Schmidt numbers greater than one (Figure 4).

From the point of view of convective diffusion theory, the high Schmidt number problem is fascinating in that different regions of the concentration field are characterized by radically different length scales, and these regions develop essentially without cognizance of each other.

The classical problem of an infinite disk rotating in an infinite body of quiescent fluid was first treated by von Karman (1921) and later by Cochran (1934). By a similarity transformation, the complete Navier-Stokes equations are reduced to a set of ordinary differential equations for which a solution is readily obtained. The same technique was employed by Bödewadt (1940) to obtain a solution of the boundary layer equations for the problem of an unbounded fluid rotating against an infinite stationary surface.

Millsaps and Pohlhausen (1952) examined heat transfer from a rotating disk for Prandtl numbers in the vicinity of unity, and exact solutions for the limits of very low and very high Prandtl numbers were obtained by Sparrow and Gregg (1959). The latter case has been concisely summarized in terms of the mass transfer analogue by Levich (1962).

Heat or mass transfer from a rotating fluid to a stationary surface has not been studied in any depth. The problem is not amenable to the same similarity transformation which is successful for the rotating disk. Consequently, the complete two dimensional convective diffusion equation must be solved, and the problem provides an interesting theoretical case study of the interaction of convection and diffusion. Furthermore, the problem is motivated by a number of practical applications wherein the Bödewadt velocity field applies over a significant portion of a stationary surface (Dorfman, 1963; Mack, 1962 and 1963). In a companion paper (Colton and Smith, 1972), the theoretical analysis developed herein is applied to the problem of mass transfer from the base of an unbaffled cylindrical tank which is agitated by an axially-mounted impeller.

VELOCITY FIELD

For an unbounded fluid rotating with an angular velocity ω against an infinite stationary surface, the equations of motion and the boundary conditions are much the same as those for the rotating disk. However, at large distances from the boundary, the centrifugal force and radial pressure gradient are balanced but nonzero. By virtue of the no slip condition, the circumferential velocity and thus the centrifugal force approach zero at the surface of the disk, whereas the radial pressure gradient is essentially independent of distance from the surface. As a result, a pressure-driven radial flow which is directed towards the axis of rotation occurs near the wall and gives rise to an axial outflow, as required by continuity.

The equations of motion are reduced to a set of ordinary differential equations by assuming the following familiar forms for the velocity components (see Figure 1 for coordinate system):

$$V_r = r\omega F(\zeta) \qquad V_\phi = r\omega G(\zeta) \qquad V_z = \sqrt{\nu\omega}H(\zeta) \quad (1)$$

where the similarity variable is defined by

$$\zeta = z\left(\frac{\omega}{\nu}\right)^{1/2} \quad (2)$$

Bödewadt (1940) obtained a solution to the boundary layer equations, and details of the solution and the velocity component profiles may be found in standard texts (Schlichting, 1960; Dorfman, 1963; Greenspan, 1968).

The axial and circumferential velocity components are always positive, and the radial component is negative near the surface. As ζ increases the flow components oscillate in magnitude before reaching their asymptotic values. The radial component alternates between inflow and outflow, although inflow predominates. The oscillations are caused by interaction of the centrifugal and Coriolis $(-\rho V_r V_\phi/r)$ forces in the circumferential momentum equation. The latter, with a negative radial velocity, accelerates flow in the ϕ direction to the point where V_ϕ is greater in regions of the boundary layer than in the free stream. The associated centrifugal force thus exceeds the radial pressure gradient and causes radial flow reversal. This in turn changes the sign of the Coriolis force so as to retard the circumferential velocity and lowers the axial velocity by continuity. The overshoot phenomenon is damped out in the free stream as all velocity components become constant, namely, $F(\infty) = 0$, $G(\infty) = 1$, $H(\infty) = \text{const.}$

The oscillatory behavior leads logically to a useful subdivision of the velocity field. For future reference we here define the *near field* $(0 < \zeta \lesssim 3)$ wherein the radial velocity component is always negative and the other components increase monotonically with distance, the *far field* $(\zeta \gtrsim 15)$ in which the velocity components have reached their asymptotic value, and the *oscillatory region* $(3 \lesssim \zeta \lesssim 15)$. The momentum boundary layer thickness, defined as the height for which the deviation of the circumferential velocity from the free stream value is less than 2%, is given by $\zeta \simeq 8$. In contradistinction, all velocity components on a rotating disk change monotonically with distance, and the boundary layer thickness is $\zeta \simeq 4$. The monotonic behavior follows from the uniformly negative direction of the Coriolis force, and the latter contrast is physically reasonable in view of the difference in direction of the axial flow.

The classical similarity solutions for both the rotating

disk and rotating fluid are strictly valid for an infinite surface, whereas any surface of practical interest is finite. This is not a serious problem for the rotating disk at high rotational Reynolds numbers because end effects are confined to a radial region the extent of which is the same order of magnitude as the thickness of the momentum boundary layer. This does not hold, however, for the case of a fluid rotating against a stationary finite disk. Here one must contend with developing velocity profiles at the leading (circular) edge of the disk, and the attractively simple velocity profiles of Equation (1) no longer apply. However, the available approximate analyses (Mack, 1962 and 1963; Rogers and Lance, 1964; Rott and Lewellen, 1966) show that the Bödewadt solution applies rigorously in the region near the axis of rotation and that it is an adequate representation over a large portion (roughly the inner half) of the disk. Hence, there follows little loss in generality if the mass transfer surface is limited to that portion of a finite disk where the similarity solution applies. Particularly with regard to understanding the physical phenomena, this suggests that the simple Bödewadt profiles are appropriate for this initial analysis.

PROBLEM STATEMENT

The system considered in this study (see Figure 1) consists of a dilute solution of constant physical properties which undergoes solid body rotation at a large distance from an infinite stationary surface and which transfers mass to or from a finite disk of radius b on that surface. We restrict our attention to large rotational Reynolds numbers, based upon the radius of the active disk ($Re = \omega b^2/\nu$), such that the momentum boundary layer thickness is small compared to the disk radius ($Re^{1/2} >> 1$). The problem is to find the concentration field in the fluid and the mass flux at the disk surface.

The convective diffusion equation for the case of axial symmetry is

$$V_r \frac{\partial c}{\partial r} + V_z \frac{\partial c}{\partial z} = D\left\{\frac{\partial^2 c}{\partial z^2} + \frac{1}{r}\frac{\partial}{\partial r}\left(r\frac{\partial c}{\partial r}\right)\right\} \tag{3}$$

and the boundary conditions of interest are

$$1.\quad 0 \leq z \leq \infty \qquad r = 0 \qquad \frac{\partial c}{\partial r} = 0 \tag{4}$$

$$2.\quad 0 < z \leq \infty \qquad r \to \infty \qquad c \to c_z \tag{5}$$

$$3.\quad z \to \infty \qquad 0 \leq r \leq \infty \qquad c \to c_\infty \tag{6}$$

$$4.\quad z = 0 \qquad b < r \leq \infty \qquad \frac{\partial c}{\partial z} = 0 \tag{7}$$

$$5a.\quad z = 0 \qquad 0 \leq r \leq b \qquad c = c_w \tag{8a}$$

$$\text{or b.}\quad z = 0 \qquad 0 \leq r \leq b \qquad -D\frac{\partial c}{\partial z} = n_0$$

$$\text{or c.}\quad z = 0 \qquad 0 \leq r \leq b \qquad -D\frac{\partial c}{\partial z} = 2P_m(c_m - c_0) \tag{8c}$$

The first boundary condition specifies symmetry about the axis of rotation. The second and third impose uniform ambient concentration at infinite distance from the transferring surface. The fourth boundary condition requires that the surface be inert for all radii greater than that of the disk. Boundary conditions (5a) and (5b) clearly

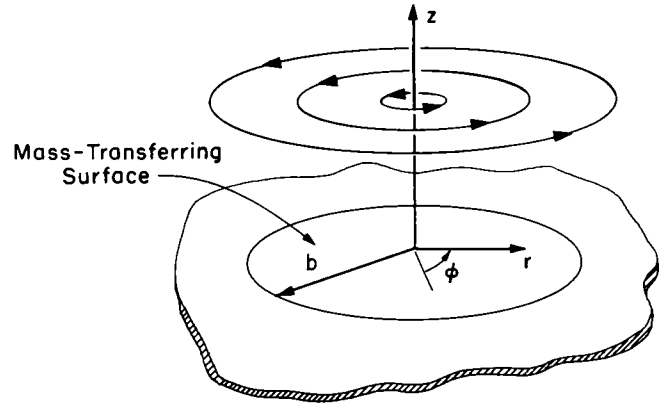

Fig. 1. Coordinate system for mass transfer from a rotating fluid to a finite disk (radius b) on an infinite stationary surface.

demand that the disk provide either a surface of uniform concentration or a surface of uniform flux, respectively. Another case of physical interest (Colton and Smith, 1972) arises if the disk is thought to be a membrane of diffusive permeability P_m which is bounded on the other side by an identical rotating fluid. In this case, the system becomes symmetrical about a plane through the center of the membrane, and the concentration in this plane is constant. The resulting boundary condition is given by Equation (8c) in which c_m is the concentration in the center plane of the membrane divided by the membrane-external fluid partition coefficient and c_0 is the concentration in the fluid at the membrane surface.

The limit $b \to \infty$ reduces this problem to the trivial solution $c = c_w$ for all $z, r \geq 0$, whereas no such difficulties are posed by this limit for the case of a rotating disk. This distinction between the rotating disk and rotating fluid follows intuitively and is qualitatively consistent with the difference between the steady state solutions for normal and reverse stagnation flows (Chan and Scriven, 1970), respectively. Hence, a finite transferring surface is the only case of physical interest, the interesting paper by Lugt and Schwiderski (1965) notwithstanding.

In dimensionless form the problem becomes

$$xF\frac{\partial \theta}{\partial x} + H\frac{\partial \theta}{\partial \zeta} = \frac{1}{Sc}\left\{\frac{\partial^2 \theta}{\partial \zeta^2} + \frac{1}{Re}\left[\frac{1}{x}\frac{\partial}{\partial x}\left(x\frac{\partial \theta}{\partial x}\right)\right]\right\} \tag{9}$$

$$1.\quad 0 \leq \zeta \leq \infty \qquad x = 0 \qquad \frac{\partial \theta}{\partial x} = 0 \tag{10}$$

$$2.\quad 0 < \zeta \leq \infty \qquad x \to \infty \qquad \theta \to 0 \tag{11}$$

$$3.\quad \zeta \to \infty \qquad 0 \leq x \leq \infty \qquad \theta \to 0 \tag{12}$$

$$4.\quad \zeta = 0 \qquad 1 < x \leq \infty \qquad \frac{\partial \theta}{\partial \zeta} = 0 \tag{13}$$

$$5a.\quad \zeta = 0 \qquad 0 \leq x \leq 1 \qquad \theta = 1 \tag{14a}$$

$$\text{or b.}\quad \zeta = 0 \qquad 0 \leq x \leq 1 \qquad -\frac{\partial \Phi}{\partial \zeta} = 1 \tag{14b}$$

$$\text{or c.}\quad \zeta = 0 \qquad 0 \leq x \leq 1 \qquad -\frac{\partial \theta}{\partial \zeta} = Sh_w(1 - \theta_w) \tag{14c}$$

The dimensionless concentration in Equation (14b) has been redefined for convenience as $\Phi = Re^{1/2}\, D\, \theta(c_w - c_z)/(n_0 b)$. When this boundary condition is applicable,

θ in Equation (9) is replaced by Φ. The wall Sherwood number Sh_w of Equation (14c) is proportional to the ratio of the mass transfer resistance in the fluid to that in the wall. As has been established (Colton et al., 1971) for boundary conditions of this nature, $Sh_w = \infty$ is equivalent to a constant concentration boundary condition, and $Sh_w = 0$ is equivalent to a constant flux boundary condition.

In this study, numerical solutions of Equation (9) are obtained with slightly modified boundary conditions, and limiting analytical solutions are derived by various techniques for regions of the concentration field where one or more terms in Equation (9) are approximately or identically zero. These solutions serve to complement and supplement the numerical solution as well as to elucidate the underlying physics.

NUMERICAL SOLUTION

Equation (9) was solved numerically on a digital computer. A term of the form $\partial\theta/\partial\tau$, where $\tau = FoReSc$, was added to the equation, and the transient solution was obtained using the alternating difference implicit procedure of Peaceman and Rachford (1955). The solution was continued until θ at all points converged to a time-invariant value within a prescribed tolerance.

To accommodate a finite grid, the outer radial boundary condition was imposed at $x = x_\infty$, and the far field boundary condition was changed to read $d\theta/d\zeta = 0$ and was imposed at $\zeta = \zeta_\infty$. This change is compatible with the boundary layer approximation and with the marked disparity between the axial length scales which are appropriate to the near field and far field regions (see below). Thus, the boundary conditions actually employed were

$$2a. \quad 0 < \zeta \leq \zeta_\infty \qquad x = x_\infty \qquad \theta = 0 \tag{15}$$

$$3a. \quad \zeta = \zeta_\infty \qquad 0 \leq x \leq x_\infty \qquad \frac{d\theta}{d\zeta} = 0 \tag{16}$$

Relatively equal accuracy over the entire field was attained with equally spaced grid points in a transformed coordinate, $y = \ln(\zeta + 1)/\ln(\zeta_\infty + 1)$, $0 \leq y \leq 1$. All results reported are for $x_\infty = 1$. This is tantamount to ignoring leakage by radial diffusion to the region $x > 1$, an assumption which is appropriate for moderate to high Schmidt numbers with the high Reynolds numbers considered here.

Mass transfer coefficients were calculated from the concentration gradients at the wall, as defined in dimensionless form by

$$St\ Sc\ Re^{1/2} = -\left(\frac{\partial\theta}{\partial\zeta}\right)_{\zeta=0} \tag{17}$$

An initial progression of time steps was employed to ensure stability. Convergence of the steady state solution was tested by standard procedures; a 50×50 grid was judged satisfactory. Additional details are available elsewhere (Colton, 1969).

ANALYTICAL SOLUTIONS

We focus here upon regions of the concentration field which are amenable to approximate analytical solution and for which the numerical solution yields reduced accuracy or is unattainable. These solutions are valid over a surprisingly large range of Schmidt numbers. The exceptions are dealt with separately below.

Leading Edge

Consider the leading edge of the disk where the concentration boundary layer initially develops (see Figure 2a). Near the wall, the radial and axial velocity components may be approximated by their Maclaurin series expansions. Since $F(0) = H(0) = H'(0) = 0$ and $H''(0) = -2F'(0)$, as required by the velocity boundary conditions and the continuity equation, these become

$$F(\zeta) = F'(0)\zeta + \frac{1}{2}F''(0)\zeta^2 + \ldots \tag{18}$$

$$H(\zeta) = -F'(0)\zeta^2 + \frac{1}{6}H'''(0)\zeta^3 + \ldots \tag{19}$$

For large values of Schmidt number, the effects of mass transfer near the leading edge are confined to a thin region near the wall which is small compared to the momentum boundary layer thickness, and we may approximate F and H by the first term in their respective series expansions. Combining Equations (1), (18), and (19) with Equation (3) leads to

$$r\omega\, F'(0)\zeta\frac{\partial c}{\partial r} - \sqrt{\nu\omega}\, F'(0)\zeta^2\frac{\partial c}{\partial z} = D\left\{\frac{\partial^2 c}{\partial z^2} + \frac{1}{r}\frac{\partial}{\partial r}\left(r\frac{\partial c}{\partial r}\right)\right\} \tag{20}$$

where, from Bödewadt (1940), $F'(0) = -0.94197$. If attention is restricted to the region $b - r << b$, comparison of the radial convection and axial diffusion terms yields a trial similarity variable

$$\chi = \frac{z}{\delta_c} = \left[-\frac{F'(0)}{9}\right]^{1/3}\left(\frac{z}{b}\right) Re^{1/2}\, Sc^{1/3}\left[\ln\left(\frac{1}{x}\right)\right]^{-1/3} \tag{21}$$

where $\ln(1/x)$ has been substituted for $(1 - x)$ to obtain a modest improvement in the solution away from the immediate leading edge and the form has been improved by a posteriori adjustment. At this point, the approaches for constant concentration and constant flux boundary conditions diverge.

Equation (20), when expressed in terms of χ, may be reduced to an ordinary differential equation if the axial convection and radial diffusion terms are negligible. This limits the region of validity of the solution to $\ln(1/x) << 1$, that is, roughly the outer 10% of the disk, and to $ReSc^{2/3}\,[\ln(1/x)]^{4/3} >> 1$. The latter constraint is not severe except in the immediate vicinity of the leading edge. Equation (20) now becomes

$$\theta'' + 3\chi^2\,\theta' = 0 \tag{22}$$

with boundary conditions $\theta(0) = 1$ and $\theta \to 0$ as $\chi \to \infty$, which leads to

$$\theta = 1 - \frac{\gamma\left(\frac{1}{3}, \chi^3\right)}{\Gamma\left(\frac{1}{3}\right)} \tag{23}$$

The local and area-averaged dimensionless mass transfer coefficients become, respectively,

$St\ Sc^{2/3}\ Re^{1/2}$

$$= \frac{1}{\Gamma\left(\frac{4}{3}\right)} \left[-\frac{F'(0)}{9} \right]^{1/3} \left[\ln\left(\frac{1}{x}\right) \right]^{-1/3}$$

$$= 0.528 \left[\ln\left(\frac{1}{x}\right) \right]^{-1/3} \quad (24)$$

and

$$\overline{St}\, Sc^{2/3}\, Re^{1/2} = 2^{1/3} \frac{\Gamma\left(\frac{2}{3}\right)}{\Gamma\left(\frac{4}{3}\right)} \left[-\frac{F'(0)}{9} \right]^{1/3} = 0.901 \quad (25)$$

Note that the dependence of the mass transfer coefficient upon Sc and Re in the leading edge region is the same as that found for the rotating disk at high Sc (Sparrow and Gregg, 1959).

If the disk provides a surface of uniform flux rather than one of uniform concentration, then Equation (14b), $-d\Phi/d\zeta = 1$, replaces the constraint that $\theta(0) = 1$. In this case, it proves convenient to define

$$\Phi = \left[-\frac{F'(0)}{9} \right]^{-1/3} Sc^{-1/3} \left[\ln\left(\frac{1}{x}\right) \right]^{1/3} f(\chi) \quad (26)$$

and if axial convection and radial diffusion are once again neglected, Equation (20) becomes

$$f'' + 3\chi^2 f' - 3\chi f = 0 \quad (27)$$

subject to $-f'(0) = 1$ and $f \to 0$ as $\chi \to \infty$. The solution is

$$f = \left\{ \frac{e^{-\chi^3}}{\Gamma\left(\frac{2}{3}\right)} - \chi \left\{ 1 - \frac{\gamma\left(\frac{2}{3}, \chi^3\right)}{\Gamma\left(\frac{2}{3}\right)} \right\} \right\} \quad (28)$$

The local dimensionless mass transfer coefficient is now given by

$$St\, Sc\, Re^{1/2} = \frac{1}{\Phi(0)} \quad (29)$$

or

$$St\, Sc^{2/3}\, Re^{1/2} = \Gamma\left(\frac{2}{3}\right) \left[-\frac{F'(0)}{9} \right]^{1/3} \left[\ln\left(\frac{1}{x}\right) \right]^{-1/3}$$

$$= 0.638 \left[\ln\left(\frac{1}{x}\right) \right]^{-1/3} \quad (30)$$

The ratio of the mass transfer coefficient between the constant flux and constant concentration boundary conditions is thus simply $\Gamma\left(\frac{2}{3}\right) \Big/ \Gamma\left(\frac{4}{3}\right) = 1.209$, as is typical of Leveque-type solutions (Colton, et al., 1971).

Far Field

Consider the concentration field far from the surface. Beyond the momentum boundary layer the axial velocity is constant and the radial velocity is negligible, in which case the radial convection term vanishes. Both axial convection and diffusion act in the same direction, depletion occurring only by radial diffusion. Furthermore, axial convection will be dominant relative to axial diffusion if $Sc\ \zeta >> 1$ (or $Sc\ Re^{1/2}\ z/b >> 1$), as may be shown by examination of Equation (3). In this case, mass will be carried far from the transferring surface and the axial length scale will be far greater than the radial length scale. This suggests an asymptotic analysis characterized by a diffusion length scale δ_c' which is akin to a boundary layer thickness (see Figure 2b).

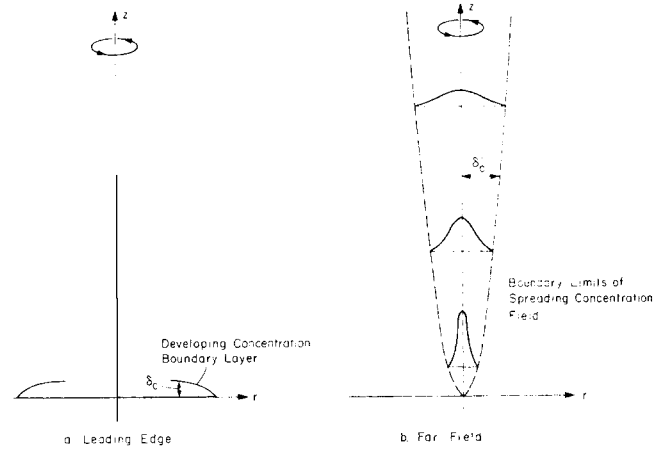

Fig. 2. Nature of approximate analytical solutions.

The convective diffusion equation now becomes, in dimensionless form,

$$H(\infty) \frac{\partial\theta}{\partial\zeta} = \frac{1}{Sc\, Re} \left[\frac{1}{x} \frac{\partial}{\partial x} \left(x \frac{\partial\theta}{\partial x} \right) \right] \quad (31)$$

which suggests the similarity variable

$$\eta = \frac{r}{\delta_c'} = Re^{1/4}\, Sc^{1/2} \frac{x}{(z/b)^{1/2}} \quad (32)$$

A similarity transformation for θ may be found by imposing the steady state compatibility condition that the mass transported through a plane perpendicular to the axis of rotation must be independent of z and equal to the total mass transfer rate:

$$N = \int_0^\infty \left[V_z(c - c_\infty) - D \frac{\partial c}{\partial z} \right] 2\pi r dr = \text{constant} \quad (33)$$

If axial diffusion is neglected relative to axial convection in the far field, this becomes

$$\overline{St}\, Sc\, Re = 2\, H(\infty) \int_0^\infty \theta \frac{z}{b} \eta\, d\eta \quad (34)$$

which suggests a similarity transformation of the form

$$\theta = A\, \overline{St}\, Sc\, Re \frac{g(\eta)}{z/b} \quad (35)$$

where A is an adjustable parameter to be determined from Equation (34) once $g(\eta)$ is known. Substitution for θ in Equation (31), followed by rearrangement, yields

$$\frac{d}{d\eta} \left[\frac{1}{\eta} \frac{dg}{d\eta} \right] + \frac{1}{2} H(\infty) \frac{d}{d\eta} [\eta^2 g] = 0 \quad (36)$$

subject to $g'(0) = 0$ and $g(\eta) \to 0$ as $\eta \to \infty$. Repeated integration gives

$$g(\eta) = B \exp\left[-\frac{H(\infty)}{4} \eta^2 \right] \quad (37)$$

Equations (34), (35), and (37) now yield $AB = 1/4$, whence

$$\theta = \frac{\overline{St}\ Sc\ Re}{4(z/b)} \exp\left[-\frac{H(\infty)}{4} Re^{1/2}\, Sc \frac{x^2}{(z/b)} \right] \quad (38)$$

where $\overline{St}$ is to be evaluated from the results of the numerical solution, and, from Bödewadt (1940), $H(\infty) \simeq$

1.35. The shape of the concentration profile is seen to be a function of both r and z, whereas the amplitude is dependent on z alone. Equation (38) is the solution for a point source of finite strength and thus may adequately represent a real source of finite area only if $\theta << 1$.

The above analysis is appropriate to the physical problem described at the outset of this paper. However, the numerical problem has been solved subject to Equation (15) and with x_s set equal to unity. For reasons to be developed below, this modified boundary condition is thought to have little effect upon the prediction of the mass transfer rate. It can have a substantial effect upon the details of the far field but not on the underlying fact of a balance between axial convection and radial diffusion therein.

For the purpose of illustrating the physical behavior and for comparison with the numerical solution, an analytical far field solution has also been developed subject to Equation (15) with $x_s = 1$. The other boundary condition has been taken as

$$\zeta - \zeta_0 = 0 \qquad 0 \leq x \leq 1 \qquad \theta = \theta(\zeta_0, x) \tag{39}$$

where ζ_0 is an arbitrarily selected plane at the base of the far field region and $\theta(\zeta_0, x)$ is to be determined from the numerical solution. As posed, the problem is formally equivalent to obtaining the transient solution for the temperature of an infinitely long cylinder having uniform initial temperature $\theta(\zeta_0, x)$ which undergoes a step change in the temperature at the surface to zero (Carslaw and Jaeger, 1959). By inspection one obtains

$$\theta(\zeta - \zeta_0, x) = \sum_{n=1}^{\infty} a_n \exp\left[-\frac{\lambda_n^2(\zeta - \zeta_0)}{H(\infty)Sc\,Re}\right] J_0(\lambda_n x) \tag{40}$$

where

$$a_n = 2\frac{\int_0^1 x\,\theta(\zeta_0, x)J_0(\lambda_n x)\,dx}{J_1^2(\lambda_n)} \tag{41}$$

In practice $\theta(\zeta_0, x)$ was evaluated at $\zeta_0 = 20$.

Low Schmidt Number

If as $Sc \to 0$, $Re^{1/2}\,Sc$ remains large compared to unity, a balance between convection and diffusion is still maintained over the entire concentration field. Furthermore, the far field solution retains its validity subject to the constraints described above. However, if both Sc and $Re^{1/2}\,Sc$ approach zero, the concentration field near the disk is determined solely by diffusion, and (Carslaw and Jaeger, 1959)

$$\frac{kb}{D} \to \frac{4}{\pi} \tag{42}$$

for a disk of uniform concentration with ambient concentration imposed at infinity. This asymptotic result has been obtained in the region near the axis of rotation by numerical solution for $Sc = 10^{-3}$, $Re = 10^4$.

RESULTS AND DISCUSSION

Unless otherwise specified, all results were obtained for $Re = 10^4$.

Mass Transfer Coefficients

Local Stanton numbers for a disk which provides a surface of uniform concentration are shown in Figure 3 as a function of radial position. The mass transfer coefficient is infinite at the leading edge and decreases monotonically to the axis of rotation, emphasizing the highly nonuniform accessibility of the surface. The radial variation is seen to be nearly independent of Schmidt number for $Sc \geq 10$. The leading edge solution is good to within 10% down to $x \simeq 0.8$ for high Schmidt numbers and is valid over progressively more limited regions as Sc decreases with Re fixed. The high Schmidt number asymptote for the rotating disk (Sparrow and Gregg, 1959)

$$St\,Sc^{2/3}\,Re^{1/2} \simeq 0.62 \tag{43}$$

is shown for comparison. The leading edge solution is seen to cross the numerical solution at $x \tilde{>} 0.95$. It is reasonable to assume that the former solution is a better representation in this region because the numerical grid is uniform in x and is therefore too coarse to represent adequately the very large and rapidly changing radial gradients which occur in the immediate vicinity of the leading edge. This leads to a modified procedure for calculating the area-averaged Stanton number. Denoting the point where the solutions intersect as x_1, use of Equation (24) leads to

$$\overline{St}\,Sc^{2/3}\,Re^{1/2} = 2\left\{\frac{1}{Sc^{1/3}}\int_0^{x_1}\left(-\frac{\partial\theta}{\partial\zeta}\right)_{\zeta=0} x\,dx\right.$$

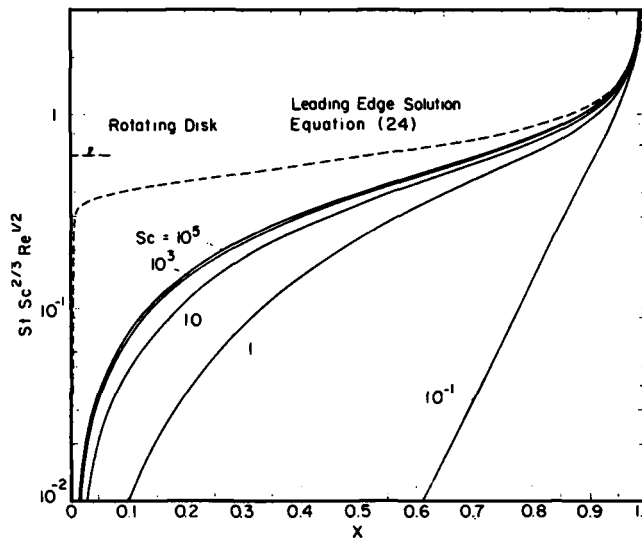

Fig. 3. Dimensionless local mass transfer coefficients as a function of radial position.

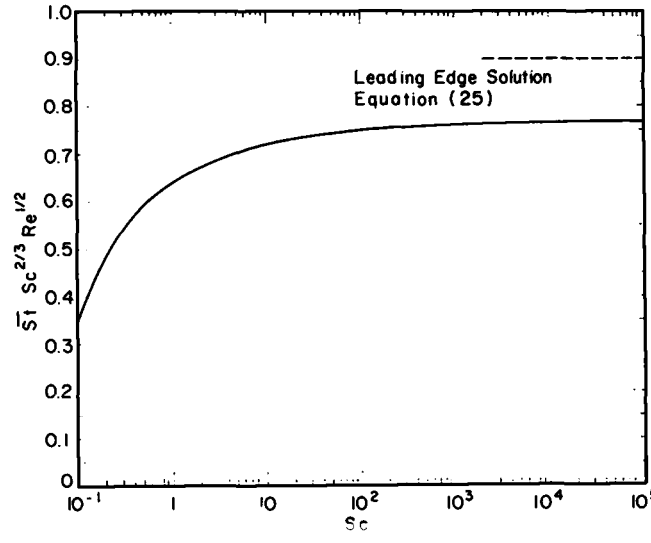

Fig. 4. Dependence of average mass transfer coefficient on Schmidt number.

$$+ 0.528 \int_{x_1}^{1} \frac{x}{\left[\ln\left(\frac{1}{x}\right)\right]^{1/3}} dx \Bigg\} \quad (44)$$

The first integral is obtained from the numerical solution and the second may be integrated by parts to obtain a finite value. The results of these calculations are shown in Figure 4. For a very high Schmidt number, the following asymptotic expression obtains

$$Sc \to \infty \qquad \overline{St}\, Sc^{2/3}\, Re^{1/2} \to 0.768 \qquad (45)$$

Equation (45) is valid with only a small change in the coefficient down to surprisingly low ($Sc \sim 1$) Schmidt numbers. Furthermore, the fact that the average mass transfer coefficient is greater for the rotating fluid than for the rotating disk is at first surprising in view of the influence of the direction of convection normal to the surface (Chan and Scriven, 1970). The reason becomes apparent upon closer inspection of Figure 3. Although the local Stanton number over the inner 70% of the stationary disk is smaller than on the rotating disk, the values near the leading edge are markedly higher. This, and the greater weighting given to this region, accounts for the higher average value and for the fact that the leading edge solution, Equation (25), predicts an average Stanton number less than 20% higher than the actual value. The relative importance of the leading edge in the overall transport process is apparent when one calculates that half the total transport takes place on the outer 15% of the disk and only 10% occurs on the inner half. It is also now apparent that for these examples the computed mass transfer coefficient should be essentially independent of the value of x_e at which the radial boundary condition is imposed.

The effect of a permeable wall boundary condition on the local Stanton number for $Sc = 10^3$ is presented in Figure 5. The curve for $Sh_w = \infty$ is the same as that for the constant concentration boundary condition in Figure 3. As expected, Stanton number increases uniformly with decreasing wall Sherwood number. The leading edge solution for a constant flux boundary condition compares favorably with the numerical solution for $Sh_w = 10^{-1}$ in the region of mutual validity. Although the ratio of the two limiting analytical solutions for Stanton number is independent of x, it is clear that this ratio actually becomes progressively larger as x decreases. The behavior of the average Stanton number is shown in Figure 6 where $\phi(Sh_w)$, the ratio of the average mass transfer coefficient at finite Sh_w to the value at $Sh_w = \infty$,

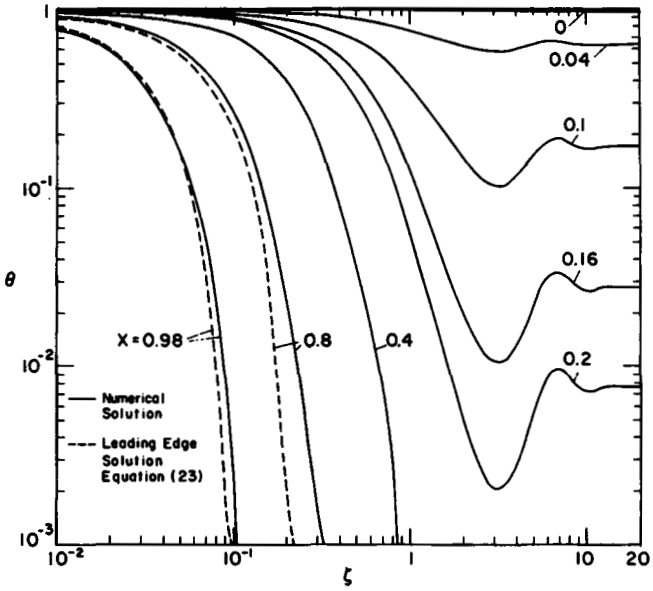

Fig. 7. Concentration field for $Sc = 10^3$.

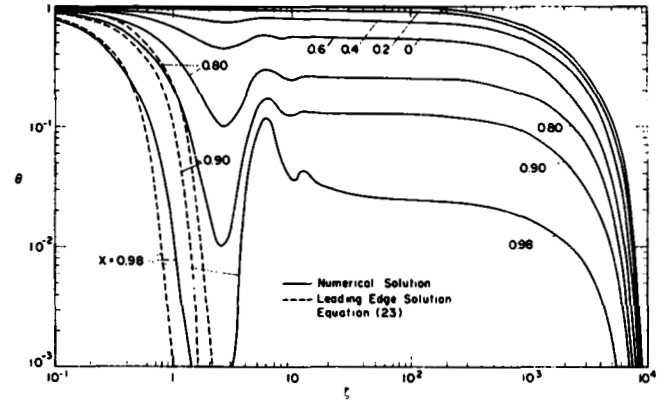

Fig. 8. Concentration field for $Sc = 1$. Numerical solution for $\tau = 2040$.

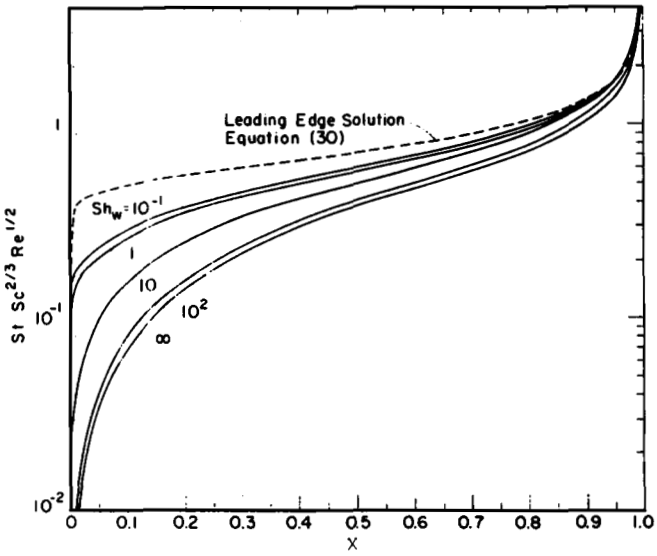

Fig. 5. Dimensionless local mass transfer coefficients as a function of radial position for a permeable wall boundary condition, Equation (14c). $Sc = 10^3$.

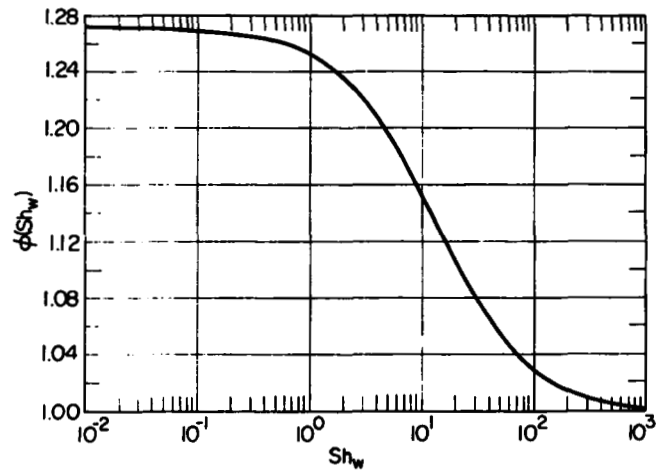

Fig. 6. Ratio of average mass transfer coefficient at finite Sh_w to value at $Sh_w = \infty$.

is plotted versus Sh_w. As $Sh_w \to 0$, $\phi(Sh_w)$ tends to an asymptotic value of 1.262.

Concentration Field

The concentration field obtained from the numerical and leading edge solutions is shown for $Sc = 10^3$ and 1, respectively, in Figures 7 and 8. (No perceptible difference was observed with a Reynolds number variation of 10^3 to 10^5 at $Sc = 10^3$.) Concentration decays sharply with increasing ζ near the leading edge but changes very slowly near the axis of symmetry. Within its region of validity, the leading edge solution is seen to agree remarkably well with the numerical solution. Large-scale oscillations in concentration occur within the region of oscillatory flow, and the maxima and minima correspond to points of radial flow reversal. The oscillations are larger at fixed x, and are discernible at lower values of x, for the higher Schmidt number, as is to be expected from the greater relative importance of convection. This is easily visualized. Near the wall, dilute fluid is drawn inwards towards the axis and acquires mass by transfer from the disk. This relatively concentrated fluid is subsequently pumped outwards from the interior, giving rise to the oscillations shown.

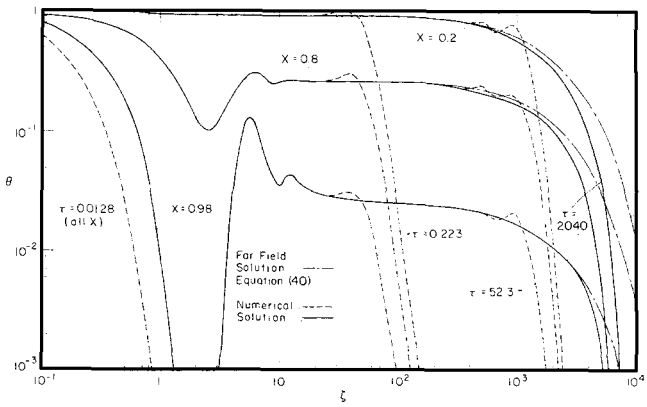

Fig. 9. Transient development of concentration field for $Sc = 1$. Solid lines ($\tau = 2040$) correspond to those in Figure 8.

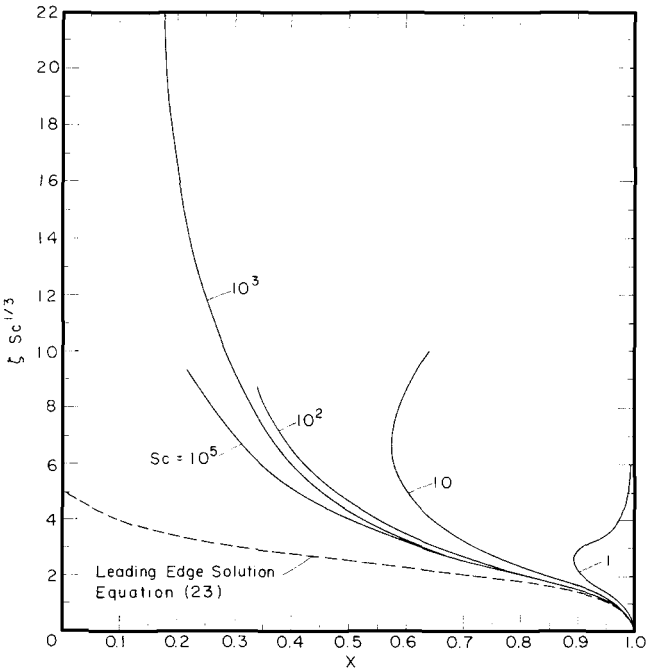

Fig. 10. Near-field boundary layer profiles, defined by $\theta = 10^{-2}$.

The transient development of the concentration field is shown in Figure 9 for $Sc = 1$. At very short times only axial diffusion is important, and the concentration field is independent of x. With increasing τ, the field penetrates into regions where axial convection dominates, and the solution propagates as a wave (with a speed equal to the axial velocity) in front of which concentration drops off sharply and behind which the field has attained its steady state value. The sharpness of the wave front is ameliorated only by axial diffusion, and the eventual attainment of steady state at all finite distances from the surface is a consequence of depletion by radial diffusion. In a sense, the mass being transported cannot "see" far ahead of itself, and the field behind the concentration wave is at its steady state. For the most part, the transient propagates almost uniformly with x, although the leading edge region reaches steady state first. This effect becomes more pronounced at high Schmidt numbers, for which markedly longer times are required in the vicinity of the axis. The modest oscillations observed at the edge of the concentration wave are doubtless spurious residual instabilities in the numerical solution. The numerical solution was arbitrarily terminated at $\tau = 2040$ after 250 time steps. Even at this very long dimensionless time, the edge of the far field had not reached steady state, as is shown in the figure by the comparison with Equation (40).

The concentration boundary layer thickness δ_c defined as the value of ζ at which $\theta = 10^{-2}$, is shown in Figure 10 for the near-field region. At high Schmidt numbers, δ_c builds up sharply at the leading edge and then increases in thickness less rapidly with decreasing x. There follows an inflection point, and the boundary layer thickness then grows more rapidly as axial convection becomes more important. The curves show that near the leading edge, the concentration field does in fact scale according to $\zeta\, Sc^{1/3}$. The multi-valued nature of δ_c is a direct consequence of the oscillations in the concentration field.

The complete envelope for $\theta = 10^{-2}$, including the far-field region, is presented in Figure 11. This is a composite plot representing various solutions, as indicated in the figure caption. The far field solution given by Equation (38) was combined with Equation (45) to yield, in modified form,

$$\theta = 0.192\, \frac{Re\, Sc^{1/3}}{\zeta} \exp\left[-0.3375\, Sc\, Re\, \frac{x^2}{\zeta}\right] \tag{46}$$

For sufficiently high values of the Schmidt number, the agreement between this simple expression and the more complex solution given by Equation (40) is striking. The far field solution is clearly insensitive to the value of x_e and to the starting condition at the edge of the oscillatory region.

CONCLUSIONS

We can now draw a coherent picture of this interactive transport process. Mass is convected predominantly radially inwards near the surface and axially upwards over the entire region. Axial diffusion acts in the same direction as axial convection, while radial diffusion acts in the opposite direction to the predominant radial convection and, in the region beyond the momentum boundary layer, acts to deplete the mass being transported axially. The net result for high Schmidt numbers is to transfer mass within the near field toward the axis of symmetry and to bring about a strong variation in the mass transfer coefficient with radial position. Beyond the momentum boundary

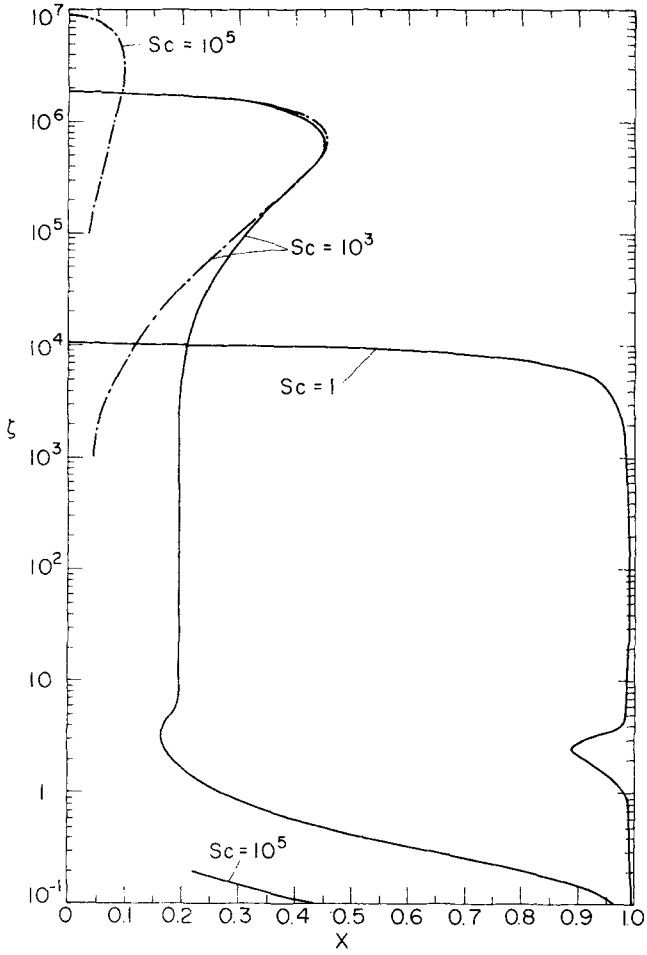

Fig. 11. Combined near- and far-field concentration profiles ($\theta = 10^{-2}$) from composite solutions. Solid line is from numerical solution for $\zeta \leq 20$ and from far field solution, Equation (40), for $\zeta \geq 20$. Intermittently dotted lines (– · – · –) are from far field solution, Equation (46).

layer, radial diffusion is so slow that an extremely long plume results. As Schmidt number decreases, the plume recedes towards the surface because radial diffusion becomes more effective in depleting the region near the axis, and the boundary layer on the transfer surface grows in thickness.

The concentration field in the near field region, which serves to establish the mass transfer rate from the surface, depends in large measure upon the gradient of the radial velocity component at the surface and is relatively insensitive to the boundary condition beyond the leading edge and to the region of oscillatory flow which lies above it. The latter, while producing interesting oscillations in the concentration field, serves primarily to establish the starting conditions for development of the far field. These conditions, however, are soon forgotten, and the concentration field at very large ζ is insensitive to the conditions near the surface and at moderate distances away from the axis. Hence, no portion of the concentration field looks far ahead, and one portion is so far removed from its origin that it does not look relatively far behind. These characteristics, in addition to the propagating-wave nature of the transient solution, lead us to conclude without too much distortion of the truth that, over selected regions of the concentration field, the mass being transferred doesn't know where it's going and may have forgotten where it came from.

ACKNOWLEDGMENTS

This study was supported in part by Contract PH 43-66-491 from the National Institute of Arthritis and Metabolic Diseases, NIH, USPHS, and by an NIH Predoctoral Fellowship to C. K. Colton. The diligent effort of Mr. H. Banijamali in evaluating and plotting the numerical data is appreciated.

NOTATION

A = numerical constant in Equation (35)
a_n = coefficient in Equation (40), defined by Equation (41)
B = numerical constant in Equation (37)
b = radius of disk which exchanges mass with fluid
c = concentration
D = molecular diffusion coefficient
F = function of ζ, dimensionless radial velocity component profile (Bödewadt, 1940)
Fo = Fourier number, Dt/b^2
f = function of χ, defined by Equation (26)
G = function of ζ, dimensionless circumferential velocity component profile (Bödewadt, 1940)
g = function of η, defined by Equation (35)
H = function of ζ, dimensionless axial velocity component profile (Bödewadt, 1940)
$J_p(x)$ = Bessel function of the first kind of order p
k = local mass transfer coefficient, $-D(\partial\theta/\partial z)_{z=0}$
$\bar{k}$ = area-averaged mass transfer coefficient
N = mass transfer rate from entire disk surface
n_0 = uniform mass flux at disk surface
P_m = membrane permeability
r = radial coordinate
Re = Reynolds number, $\omega b^2/\nu$
Sc = Schmidt number, ν/D
Sh_w = wall Sherwood number, $2 P_m \Big/ \left[D \left(\frac{\omega}{\nu} \right)^{1/2} \right]$
St = Stanton number, $k/\omega b$
$\overline{St}$ = area-averaged Stanton number, $k/\omega b$
t = time
V = velocity
x = dimensionless radial coordinate, r/b
z = axial coordinate

Greek Letters

$\Gamma(a)$ = gamma function
$\gamma(a, x)$ = incomplete gamma function
δ_c = concentration boundary layer thickness
δ_c' = characteristic length for radial diffusion near the axis of rotation
ζ = dimensionless axial coordinate, $\zeta = z(\omega/\nu)^{1/2} = (z/b)Re^{1/2}$
η = dimensionless similarity variable, defined by Equation (32)
θ = dimensionless concentration, $(c - c_x)/(c_w - c_x)$; for permeable wall boundary condition, $(c - c_x)/(c_m - c_x)$
λ_n = roots of $J_0(\lambda_n) = 0$
ν = kinematic viscosity
τ = dimensionless time, $Fo\ Re\ Sc = \omega t$
Φ = dimensionless concentration for uniform flux boundary condition, $D\ Re^{1/2}\ (c - c_x)/n_0\ b$
ϕ = circumferential coordinate
χ = dimensionless similarity variable, defined by Equation (21)
ω = angular velocity

Subscripts

m = *midplane of permeable wall*

o = arbitrary position at base of far field region, membrane surface
r = radial
w = surface of disk; wall
z = axial
ϕ = circumferential
∞ = position of far-radial or far-axial boundary condition

LITERATURE CITED

Bödewadt, V. T., "Die Drehströmung über festem Grunde," Z. *Angew. Math. Mech.*, **20**, 241 (1940).

Carslaw, H. S., and J. C. Jaeger, Conduction of Heat in Solids, 2nd Edit., Oxford University Press, Oxford (1959).

Chan, W. C., and L. E. Scriven, "Absorption into Irrotational Stagnation Flow. A Case Study in Convective Diffusion Theory," *Ind. Eng. Chem. Fundamentals*, **9**, 114 (1970).

Cochran, W. G., "The Flow Due to a Rotating Disk," *Proc. Camb. Phil. Soc.*, **30**, 365 (1934).

Colton, C. K., "Permeability and Transport Studies in Batch and Flow Dialyzers with Applications to Hemodialysis," Ph.D. thesis, Mass. Inst. Technol., Cambridge (1969).

———, K. A. Smith, P. Stroeve, and E. W. Merrill, "Laminar Flow Mass Transfer in a Flat Duct with Permeable Walls," *AIChE J.*, **17**, 773 (1971).

Colton, C. K., and K. A. Smith, "Mass Transfer to a Rotating Fluid. Part II. Transport from the Base of an Agitated Cylindrical Tank," *ibid.*, **18**, 958 (1972).

Dorfman, L. A., 'Hydrodynamic Resistance and the Heat Loss of Rotating Solids, Oliver and Boyd, London (1963).

Greenspan, H. P., The Theory of Rotating Fluids, Cambridge Univ. Press, Cambridge (1968).

von Karman, T., "Laminaire und turbulente Reibung," Z. *Angew. Math. Mech.*, **1**, 233 (1921).

Levich, V. G., Physicochemical Hydrodynamics, Prentice-Hall, Englewood Cliffs, N. J. (1962).

Lugt, H. J., and E. W. Schwiderski, "Temperature Distributions in Rotating Flows Normal to a Flat Surface," *Quart. J. Mech. Appl. Math.*, **23**, 133 (1965).

Mack, L. M., "The Laminar Boundary Layer on a Disk of Finite Radius in a Rotating Flow. Part I: Numerical Integration of the Momentum-Integral Equations and Application of the Results to the Flow in a Vortex Chamber," Jet Propulsion Lab. Techn. Rept. No. 32-224 (May, 1962).

———, "The Laminar Boundary Layer on a Disk of Finite Radius in a Rotating Flow. Part II: A Simplified Momentum-Integral Method," No. 32-366 (Jan. 1963).

Millsaps, K., and K. Pohlhausen, "Heat Transfer by Laminar Flow from a Rotating Plate," *J. Aeronaut. Sci.*, **10**, 120 (1952).

Peaceman, D. W., and H. H. Rachford, Jr., "The Numerical Solution of Parabolic and Elliptic Differential Equations," *J. Soc. Ind. Appl. Math*, **3**, 28 (1955).

Rogers, M. H., and G. N. Lance, "The Boundary Layer on a Disc of Finite Radius in a Rotating Fluid," *Quart. J. Mech. Appl. Math.*, **17**, 319 (1964).

Rott, N., and W. S. Lewellen, "Boundary Layers and Their Interactions in Rotating Flows," *Progr. Aeronaut. Sci.*, **7**, 111 (1966).

Schlichting, H., Boundary Layer Theory, 4th Edit., McGraw-Hill, N. Y. (1960).

Sparrow, E. M., and J. L. Gregg, "Heat Transfer from a Rotating Disk to Fluids of Any Prandtl Number," *J. Heat Transfer, Trans. ASME, Ser. C.*, **81**, 249 (1959).

Manuscript received November 24, 1971; revision received May 19, 1972; paper accepted May 19, 1972.

Mass Transfer to a Rotating Fluid

Part II. Transport from the Base of an Agitated Cylindrical Tank

Mass transfer to the base of an unbaffled cylindrical tank which is agitated by an axially-mounted impeller is studied experimentally and theoretically. Measured local mass transfer coefficients vary with radial position and fall within theoretical bounds derived for the case of a fluid undergoing solid body rotation above the boundary layer on the base. Average mass transfer coefficients and torque delivered to the base are fitted by consistent theoretical expressions, and an empirical correlation is developed for calculating the average liquid phase mass transfer coefficient.

CLARK K. COLTON and KENNETH A. SMITH

Department of Chemical Engineering
Massachusetts Institute of Technology
Cambridge, Massachusetts 02139

SCOPE

The stirred tank is a convenient geometry for the study of interfacial mass transport and the measurement of membrane transport properties. For example, diffusive permeability is commonly measured in a dialysis cell in which a membrane separates two identical unbaffled cylindrical chambers, each of which is agitated by an axially-mounted impeller placed in close proximity to the membrane surface. A similar arrangement may be employed, sometimes with only one chamber and a supported membrane, for the evaluation of filtration properties.

Assessment of intrinsic membrane properties is complicated by the resistance to mass transfer offered by the concentration boundary layers adjacent to the membrane. Transport of a rapidly permeating solute across a membrane may be wholly or partially rate-controlled by these boundary layers and not by the membrane at all. The usual approach is to minimize the liquid-phase resistances by intense stirring. Some workers have used a Wilson Plot method wherein measurements are made at different stirring speeds and extrapolated to infinite speed. In few instances has the average mass transfer coefficient been measured directly, and never previously in the specific